Journal of
Synchrotron Radiation

ISSN 0909-0495

Received 22 June 2009
Accepted 15 January 2010

Mercury speciation in the colloidal fraction of a soil polluted by a chlor-alkali plant: a case study in the South of Italy

A. Santoro,[a] R. Terzano,[a]* G. Blo,[b] S. Fiore,[c] S. Mangold[d] and P. Ruggiero[a]

[a]Dipartimento di Biologia e Chimica Agro-forestale e Ambientale, University of Bari, via Amendola 165/A, 70126 Bari, Italy, [b]Department of Chemistry, University of Ferrara, via L. Borsari 46, 44100 Ferrara, Italy, [c]Istituto di Metodologie per l'Analisi Ambientale, CNR-IMAA, ZI 70125 Tito Scalo, Italy, and [d]Forschungszentrum-Karlsruhe, Institute for Synchrotron Radiation, Karlsruhe, Germany. E-mail: r.terzano@agr.uniba.it

Mercury (Hg) speciation in different size fractions of a soil sample collected near an industrial area located in the South of Italy, which had been polluted by the dumping of Hg-containing wastes from a chlor-alkali plant, was investigated by XANES spectroscopy. In particular, a special procedure has been developed to study the soil colloidal fraction, both for sample preparation and for XANES data collection. In this soil, Hg was speciated in quite insoluble inorganic forms such as cinnabar (α-HgS), metacinnabar (β-HgS), corderoite ($Hg_3S_2Cl_2$), and some amorphous Hg, S and Cl-containing species, all derived from the land-disposal of K106 Hg-containing wastes. The contribution of the above-mentioned chemical forms to Hg speciation changed as a function of particle size. For the fraction <2 mm the speciation was: amorphous Hg–S–Cl (34%) > corderoite (26%) > cinnabar (20%) = metacinnabar (20%); for the fraction <2 μm: amorphous Hg–S–Cl (40%) > metacinnabar (24%) > corderoite (20%) > cinnabar (16%); and for the fraction 430–650 nm, where most of the colloidal Hg was concentrated: amorphous Hg–S–Cl (56%) > metacinnabar (33%) > corderoite (6%) > cinnabar (5%). From these data it emerged that, even if Hg was speciated in quite insoluble forms, the colloidal fraction, which is the most mobile and thus the most dangerous, was enriched in relatively more soluble species (*i.e.* amorphous Hg–S–Cl and metacinnabar), as compared with cinnabar. This aspect should be seriously taken into account when planning environmental risk assessment, since the small particle size in which Hg is concentrated and the changing speciation passing from millimetre to nanometre size could turn apparently safe conditions into more hazardous ones.

Keywords: XANES; mercury speciation; colloidal fraction; soil pollution; K106.

1. Introduction

Mercury (Hg) is one of the most dangerous global pollutants and in recent decades it has accumulated in the environment in considerable amounts mainly because of human activities (Biester *et al.*, 2000, 2007; Gray & Hines, 2006). In particular, in soil it can be present in a large variety of chemical forms, very often bound to the finest soil fractions (Roberts *et al.*, 2005). It is generally recognized that the concentration of trace pollutants tends to vary according to the particle size, with the highest amounts often concentrated in the smaller soil particles. This happens as a consequence of the higher available surface area, the higher clay mineral and organic matter content, and the more abundant presence of highly reactive Fe/Mn (hydr)oxides (Schuman, 2005). In addition, the very small soil colloidal particles (either organic or inorganic) can be more easily mobilized, thus diffusing the contaminant into other environmental compartments or endangering the health of living organisms and human beings (Slowey *et al.*, 2005).

Within this context, not only the chemical speciation of Hg, but also the determination of the size of the Hg-bearing particles in soil, is of great relevance to better assess the environmental fate and toxicity of this dangerous pollutant. In particular, the particles with a colloidal dimension (<1 μm) deserve special attention (Lead & Wilkinson, 2007).

In the present study, the distribution of Hg in the different submicrometre fractions of a soil sample collected near an industrial area located in the South of Italy and polluted by the dumping of Hg-containing wastes from a chlor-alkali plant was investigated. In particular, detailed Hg speciation was

also assessed by X-ray absorption near-edge spectroscopy (XANES) for the submicrometre fraction containing the highest amount of Hg. To perform such a speciation study, a special procedure was developed both for sample preparation and for XANES data collection.

2. Experimental

2.1. Soil sampling and characterization

For this study, a representative surface soil sample (0–10 cm depth) was selected among many others collected near the industrial area of Ferrandina (Matera, Italy) during a larger sampling campaign carried out in 2006 and 2007 (Santoro *et al.*, 2010). The investigated soil sample is sandy loam (USDA) with 2.98% of organic carbon and a pH of 8.0.

Once collected, the soil sample was homogenized, air dried, sieved at 2 mm, stored in HDPE vessels, and kept at 277 K prior to analysis.

Total Hg content was determined using an Automatic Mercury Analyser (AMA 254, FKV, Altec). A seven-step sequential extraction procedure (SEP) (Quejido *et al.*, 2002; Sánchez *et al.*, 2005) was performed on the soil sample sieved at 2 mm to determine the partitioning of Hg associated with different soil constituents and to elucidate the potential availability and mobility of Hg according to the solubilization promoted by various extracting solutions at increasing strength. Briefly, the adopted SEP enables the following operative pools to be discriminated: water-soluble (deionized H_2O); exchangeable (NH_4Cl 1 *M*); carbonates (ammonium acetate 1 *M*, pH 4.5); easily reducible (Tamm's solution); 6 *M* HCl soluble; oxidizable (H_2O_2, ammonium acetate, HNO_3 pH 2); residue (dry analysed by AMA 254).

The soil clay fraction (<2 µm) was separated by dispersing 3.5 g of soil in 50 ml of deionized water and stirring for 10 min. Then, the solution was sonicated for 10 min at 100 W by means of a Sonics Vibra-Cell (Sonics and Materials Inc., USA) to mechanically break the soil aggregates. No chemical treatment was used in order to avoid modifications in Hg speciation. After sonication, the suspension was centrifuged for 2.07 min at 600 r.p.m. by using a Model CR15 B Braun Biotech International (USA) centrifuge. The supernatant containing the clay fraction was collected and centrifuged at 5500 r.p.m. for 30 min. The final solid residue was then lyophilized using a Hetosicc (Hetolab equipment, Denmark) lyophilizer and stored at 277 K for further analysis (Terzano *et al.*, 2010).

Total Hg concentration was also determined for the clay fraction using the Automatic Mercury Analyser. Both the <2 mm and the <2 µm fractions were analysed by using scanning electron microscopy coupled to energy-dispersive spectroscopy (SEM-EDS, FESEM-SUPRA 40 Carl Zeiss AG).

2.2. Separation of the soil colloidal fraction and fractionation

The soil colloidal fraction (<1 µm) was separated by using the same procedure adopted for the clay fraction (reported above) except for the centrifugation at 600 r.p.m. which lasted for 4.13 min.

Detailed particle size distribution within the soil colloidal fraction was assessed by using the sedimentation field-flow fractionation (Sd-FFF) technique (Chittleborough *et al.*, 1992; Giddings, 1993; Blo *et al.*, 1995; Ranville *et al.*, 1999; Hassellov *et al.*, 2001).

The employed Sd-FFF apparatus was a Model S-101 SdFFF fractionator (FFFractionation, Inc., Salt Lake City, UT, USA). The fractionation channel, made up of two Hallostey C inox bars and a Mylar spacer of nominal thickness equal to 0.0254 cm, was of width 2.0 cm and length ~90 cm tip-to-tip. The channel void volume was 4.8 ml and the axis-to-channel distance was ~15 cm. A channel flow of 1.5 ml min^{-1} was generated by a Model 422 Master HPLC pump (Kontron Instruments, Italy). The carrier was Milli-Q deionized water (Millipore, Bedford, MA, USA). The sample was prepared by dispersing 50 mg of the soil sample (<1 µm fraction) in 50 ml of Milli-Q deionized water. A sample volume of 100 µl was injected for each fractionation. The outlet tube of the SdFFF system was connected to a UV detector operated at 254 nm (Uvidec 100, Jasco, Japan) and the signal was fed to a Linseis Model L6512 X-Y recorder (Linsel GmbH Selb, Germany). UV absorbance data were collected using an in-house-developed program and handled by using the FFFractionation Inc. software in order to derive the fractogram which shows the UV response profile *versus* equivalent sphere diameter (Blo *et al.*, 2006).

Ten SdFFF fractions were collected in correspondence to the following eluted sizes: <0.05 µm, 0.05–0.09 µm, 0.09–0.14 µm, 0.14–0.25 µm, 0.25–0.43 µm, 0.43–0.65 µm, 0.65–0.8 µm, 0.8–0.9 µm, 0.9–1.0 µm, 1.0–1.1 µm, and the Hg content was determined in each fraction. Taking into account the high dilution (by a factor of about 500) of the sample during the SdFFF run, five FFF runs were repeated and the relative equivalent fractions were joined together and then concentrated in an oven at 303 K for 24 h in order to obtain a detectable amount of Hg from each fraction.

Total mercury concentration in the eluted fractions, collected by using a Model 2110 collector (Bio-Rad Laboratories, Italy), was determined by off-line coupling the SdFFF instrument to an electrothermal atomic absorption spectroscopy analyzer (ETAAS) Model AAnalyst 800 (Perkin Elmer, USA). A flow injection (FI) device (FIAS 100, Perkin Elmer, USA) equipped with a Model AS800 autosampler (Perkin Elmer, USA) was used for the sample injection inside the ETAAS system. An in-house-developed mercury vapour and hydride generator apparatus (MH) allowed a lower detection limit (0.08 µg kg^{-1}) to be reached.

2.3. Sample preparation for XANES analyses: fraction 430–650 nm

The equivalent 430–650 nm fractions, obtained from five replicated SdFFF runs, were combined, concentrated by evaporation at 303 K and deposited by filtration under vacuum on a polycarbonate filter (0.2 µm pore size, Nucle-

pore, Whatman), which was then cut into 2 mm × 13 mm strips. The various strips were piled up in several layers in order to increase the Hg amount in the volume hit by the incident beam, thus increasing the Hg signal. In addition, the strips were arranged so that a horizontal sample size of 25 mm could be obtained to have a usable horizontal beam size of 16 mm. The composed sample was finally secured with Kapton tape and placed in the X-ray beam. Such a preparation ensured for an enhanced fluorescent signal by a factor of two.

In order to obtain XANES spectra with a reasonable signal-to-noise ratio, without changes on the detector system, two other improvements were developed for the purpose. (i) Use of a Cr filter: inserting a Cr metal foil as filtering material between the sample and the fluorescence detector reduced the fluorescence signal of the iron by more than 60%. Because of this action the minimum possible detector distance at the beamline could be reached. (ii) Changes in the incident angle: the influence of different angles (15°, 30°, 45° and 60°) between the incident beam and the sample on the quality of the spectra was tested. The best angle was found to be 45°. Higher angles allowed using smaller horizontal size of the incident beam. Lower angles were not efficient because of the unequal distribution of the fluorescence count rate on the different detector elements.

2.4. Synchrotron XANES analyses

XANES spectra were collected for three different fractions of the soil sample under investigation: <2 mm, <2 µm and 430–650 nm.

For comparison, XANES spectra were also acquired for a large number of Hg-standard compounds: elemental mercury, cinnabar (α-HgS, here labelled as HgS), metacinnabar (β-HgS, here labelled as m-HgS), mercury oxide (HgO), mercuric chloride ($HgCl_2$), mercurous chloride (Hg_2Cl_2), mercuric sulfate ($HgSO_4$), mercurous sulfate (Hg_2SO_4), mercury acetate, corderoite ($Hg_3S_2Cl_2$), Hg(II) bound to humic acids, Hg(II) sorbed to goethite and K106.

All the standards were purchased from Sigma-Aldrich with the following exceptions: corderoite (Mcdermitt, Nevada) which was purchased from Minerals and More (USA), Hg(II) bound to humic acids and Hg(II) sorbed to goethite which were prepared in-house.

K106 is a mercury-bearing waste material resulting from the treatment of effluents from the electrolytic process employed to generate chlorine gas and sodium hydroxide in chlor-alkali plants. This material was artificially synthesized in the laboratory and has been characterized elsewhere (Terzano *et al.*, 2010). Its composition is the following: metacinnabar 20%, halite (NaCl) 20%, α-sulfur 26% and amorphous Hg–S–Cl phases 34%.

XANES analyses were performed at the XAS beamline of the ANKA synchrotron facility (Karlsruhe, Germany). ANKA synchrotron facility operates at an electron energy of 2.5 GeV and ring currents between 70 and 170 mA.

Data were recorded around the L_{III} absorption edge of Hg at 12284 eV in fluorescence mode for soil samples and in transmission mode for Hg-standards. To reduce self-absorption effects, samples and standards were opportunely diluted with BN (Sigma-Aldrich) and pressed into discs of diameter 1.3 cm and thickness 1 mm. A Si(111) crystal pair monochromator was used for all the measurements and the monochromator was detuned to 65% of the maximum beam intensity. All scans were performed under ambient conditions with a 45° angle of the sample to the incident beam and the detector. For the fluorescence detection with a five-element germanium detector (Canberra, Olen) the peaking time of the digital detector electronic (XIA LLC, Hayward, CA, USA) was set to 500 µs. The detector window was adjusted to ±250 eV around the $L_{\alpha 1-2}$ lines. The detector-to-sample distance was minimized for each sample until an input count rate of 350.000 counts s^{-1} was reached or the detector was at the minimum distance to the sample of 40 mm. The energy was initially calibrated against the first inflection point of a gold foil (Au L_{III} 11919 eV). Thereafter, an $HgCl_2$ standard was regularly measured during the experiment, to correct any energy displacement (Bernaus *et al.*, 2005). Three scans were averaged for the Hg-standards, while five to eight scans were averaged for the soil samples.

The XAS data reduction was accomplished by using the *IFEFFIT* software package (1.2.11 version), containing *Athena*, *Artemis* and *Sixpack* softwares (Ravel & Newville, 2005; Webb, 2005).

A combination of principal component analysis (PCA), target transformation and linear combination least-square fit (LCF) of Hg L_{III}-edge soil samples spectra with the spectra of known Hg-standard compounds was used for XANES spectra analysis. From PCA results, two components were found sufficient to reconstruct all the sample spectra. To assess which standards were good candidates to be used in LCF, a spoil value was determined for the various Hg-reference compounds (Webb, 2005). Six standards gave a spoil value below 4.5 (good for 1.5–3; fair for 3–4.5; poor for 4.5–6) and were therefore used in LCF: K106 (2.2), m-HgS (2.7), Hg-goethite (3.2), $HgCl_2$ (3.4), corderoite (3.7) and HgS (3.9). The LCF was performed from 50 eV below to 115 eV above the Hg L_{III}-edge.

The quality of the LCF for the XANES spectra was evaluated by calculating the *R*-factor, which is defined as follows,

$$R = \sum_{i=1}^{N} \left(y_i^{\exp} - y_i^{\mathrm{cal}}\right)^2 \Big/ \sum_{i=1}^{N} \left(y_i^{\exp}\right)^2, \qquad (1)$$

where N is the number of data points, and $y_i^{\exp}$ and y_i^{cal} are the experimental and calculated data points, respectively.

3. Results and discussion

The total mercury concentration in soil (sieved at 2 mm) was 47 ± 6 mg kg^{-1}. Almost all Hg could be solubilized from soil only by using strong extractants such as HCl 6 *M* (82%) and H_2O_2–HNO_3 (3%) while 15% remained in the residual fraction. No mercury was extracted in the more labile fractions (water soluble, exchangeable, weak acidic conditions and

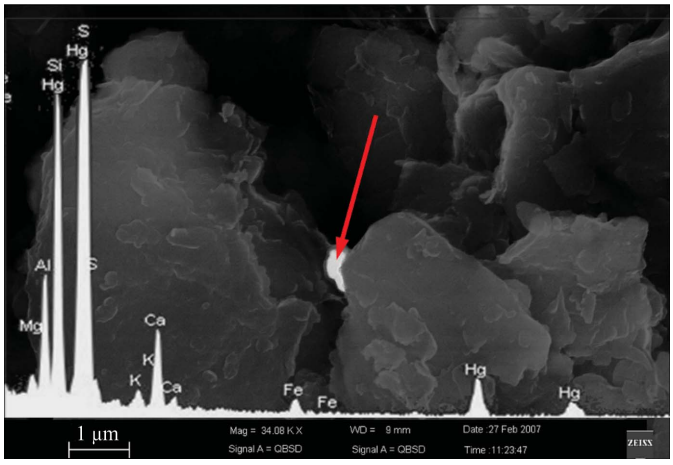

Figure 1
Micrograph and EDX spectrum for an Hg-rich particle (indicated by the arrow) in the soil sample.

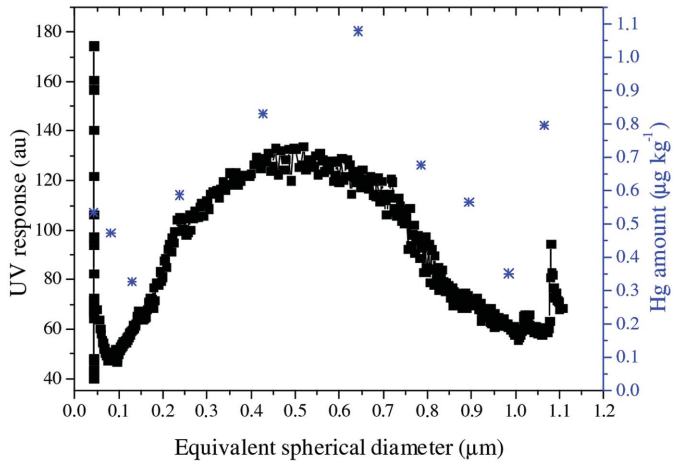

Figure 2
SdFFF fractogram for the colloidal fraction (<1 µm) of the soil sample, showing the particle size distribution (µm) against the UV detector response (a.u.) (black line and square points), and the concentration of Hg (µg kg^{-1}) in the different fractions as determined by MH–FI–ETAAS (blue star points).

complexing agents). These results suggested that Hg was most likely speciated in quite insoluble forms (*e.g.* HgS, Hg_2Cl_2, Hg^0, sorbed to crystalline Fe and/or Mn oxides *etc.*) and that soil organic matter played only a minor role in Hg complexation (only 3% is extracted in the oxidizable fraction).

SEM observations could only reveal the presence of rare very small (<1 µm) HgS particles (Fig. 1). By analysing Fe and Mn oxides by SEM-EDX, no Hg was found associated with these minerals. Microscopic observations thus suggested that most of the mercury could have been concentrated in the smaller size fractions.

Actually, after separating the clay fraction, the Hg concentration in the fraction <2 µm was found to be three times higher (148 ± 15 mg kg^{-1}) than in the overall soil sample. This result is particularly relevant from an environmental point of view since for this soil the clay fraction accounted for the 30% of the total soil dry weight, containing 81% of the total soil Hg. It is well known that very small particles can be more easily mobilized in soil as colloidal dispersions in water fluxes or in the atmosphere as airborne particles. In particular, the smaller the size, the higher the risk of diffusion of the contaminant in the environment. In this context, the so-called colloidal fraction (<1 µm) is the most active and therefore it needs to be deeply investigated. For this reason, a detailed particle size distribution in the soil colloidal fraction (<1 µm) was studied by using the Sd-FFF technique, and Hg concentration in the eluted fractions was also determined by MH–FI–ETAAS, coupled off-line with SdFFF (Contado *et al.*, 1997; Blo *et al.*, 2006).

The SdFFF fractogram of Fig. 2 obtained for the colloidal soil fraction (<1 µm) shows the size distribution (black line) of the submicrometre soil particles in the range 0.05–1 µm. The first peak around 0.05 µm could simply be an artefact from the void-time signal in the fractogram, but it could also indicate the presence of ultrafine particles, as successively confirmed by SEM investigations (not shown). In addition, SEM investigations of this fraction proved a non-significant presence of soil particles sized at higher values than 0.05 µm, showing a non-ideal elution behaviour in SdFFF fractionation because of their irregular and non-spherical shape.

The results obtained for Hg determination in each fraction are also reported in Fig. 2. From these results it emerged that most of the mercury is concentrated in the soil particles inside the dimensional range 430–650 nm and therefore this size fraction was selected for XANES analysis. The complex procedure adopted to determine Hg concentration in the different submicrometre fractions does not make straightforward an estimation of the contribution of the 430–650 fraction to the entire Hg soil content. However, from all our observations, it is reasonable to think that, despite this soil fraction representing only a tiny percent of the total soil mass, its contribution to the whole Hg amount in soil can be very high.

The significant presence of Hg in the void-time fraction (<0.05 µm) may indicate dissolved Hg forms or, most probably, simply ultrafine Hg-rich particles.

From all the data presented up to here, it appeared that the Hg concentration in the soil sample increased inversely as a function of particle size.

To determine Hg speciation in the different soil fractions, Hg L_{III} XANES spectra were collected for the soil fractions <2 mm, <2 µm and 430–650 nm (the submicrometre fraction containing the highest Hg concentration).

For the fraction 430–650 nm, a special procedure for sample preparation and data acquisition was developed, owing to the high dilution of the sample during the SdFFF run and the use of the L_{III} absorption line for Hg, which makes the analysis relatively insensitive to this element. For such a diluted sample, sample position and beamline alignment devices were also properly set up to maximize the detector performances and the fluorescent signal, as described in §2.3.

Despite all the optimization procedures adopted, the data were still quite noisy; therefore, to obtain a reasonable XANES spectrum to be used for speciation studies, 11 spectra

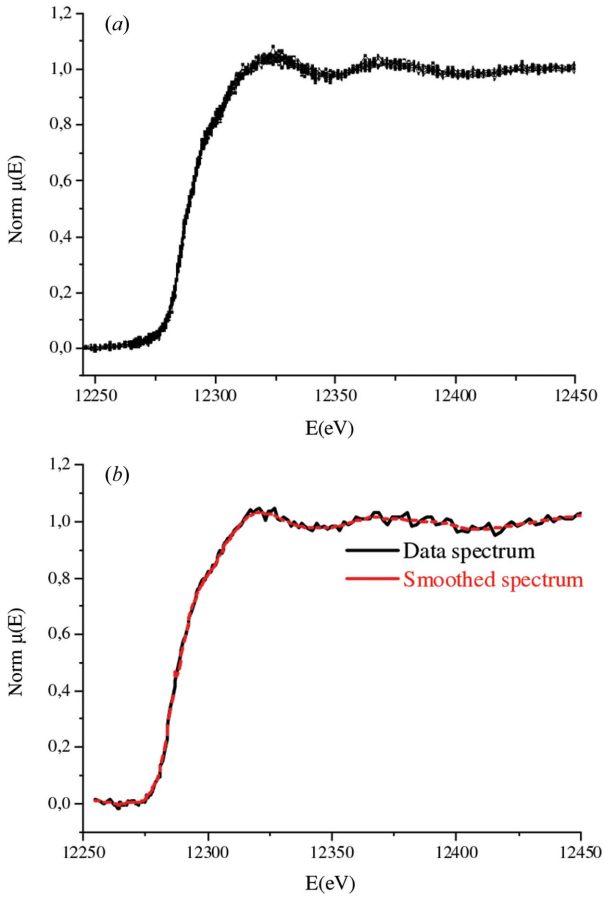

Figure 3
(*a*) Overlap of the data points for 11 Hg-XANES spectra. (*b*) Averaged spectrum (black line) and smoothed spectrum (red line) collected for the soil fraction 430–650 nm.

were collected, averaged and finally smoothed as shown in Fig. 3.

The Hg-XANES spectra obtained for the different soil fractions were fit with a linear combination of standard spectra appropriately selected among a large number of reference spectra of known compounds after performing PCA (see §2.4), and the best results for the fit are reported in Fig. 4.

In general, to fit all the experimental spectra, the following standards have been adopted: K106, cinnabar and corderoite. The choice of these three standards to fit the samples spectra was supported not only by the best *R*-factor obtained after simulating the experimental data but also by other micro-analytical studies we performed on similar soil samples (Terzano *et al.*, 2010) and by consideration of the SEM-EDX and SEP results which seem to exclude the presence of $HgCl_2$ (highly soluble) and Hg-goethite species, as suggested by PCA.

K106 is a waste sludge listed by US EPA that was produced in chlor-alkali plants using mercury cells (Castner-Kellner process), by treating Hg-contaminated wastewaters in order to precipitate mercury in the form of insoluble sulfides prior to disposal. Until 1992 the common practice was that, once filtered, this waste was land disposed (Hagemoen *et al.*, 1994). After this date, the new regulation established that K106 had

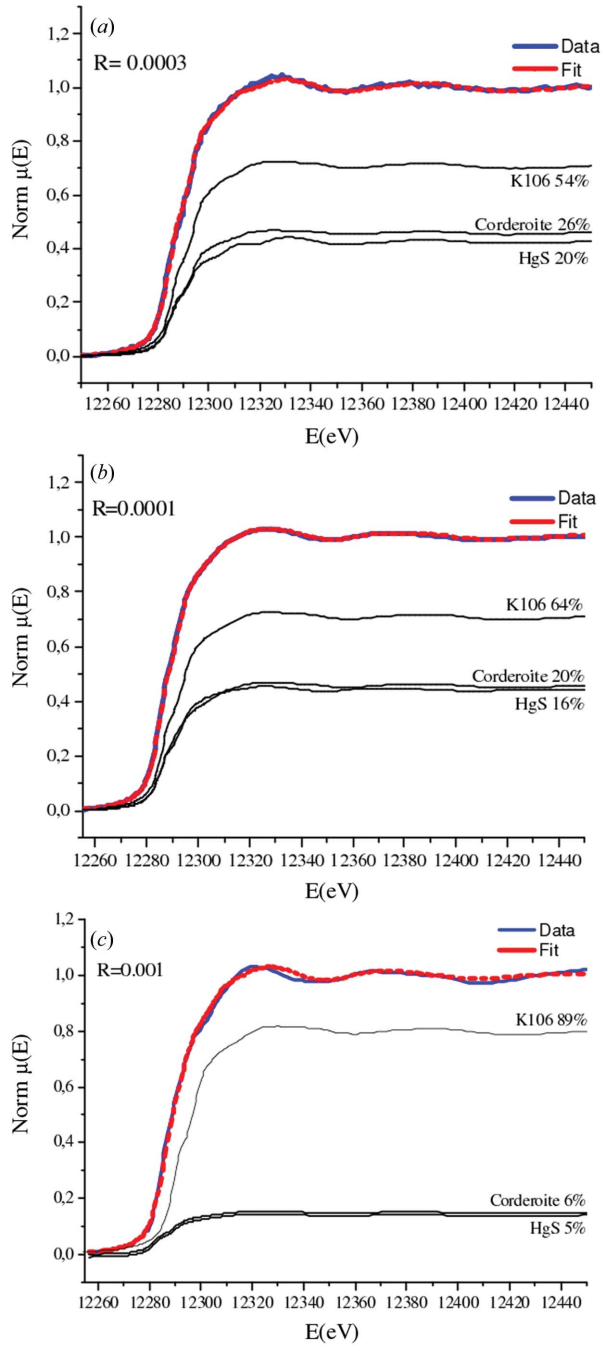

Figure 4
Linear combination fitting for the XANES spectra of the soil fractions <2 mm (*a*), <2 μm (*b*) and 430–650 nm (*c*) by using the spectra of known reference compounds. The percentage contribution of the standard spectra to the fit and *R* values are also reported.

to be thermally treated to reduce Hg content. Actually, the contamination of our investigated site dated back to the 1960s–1980s (Santoro *et al.*, 2010). By considering that the XANES data referred only to the Hg-bearing species and that the Hg phases in K106 are for the 37% m-HgS and for the 63% amorphous Hg–S–Cl (Terzano *et al.*, 2010), the complete Hg speciation in the three soil fractions could be determined as reported in Table 1.

Table 1
Hg speciation (as % in weight) for <2 mm, <2 μm and 430–650 nm soil fractions.

	Hg species (%)		
	<2 mm	<2 μm	430–650 nm
Amorphous Hg–S–Cl	34	40	56
m-HgS	20	24	33
HgS	20	16	5
Corderoite ($Hg_3S_2Cl_2$)	26	20	6

In all the soil fractions, the amorphous Hg-bearing phase accounts for the highest percentage. In the smaller fractions (<2 μm and 430–650 nm), the amount of the amorphous phase and metacinnabar increases in comparison with the other phases and in particular the contribution of cinnabar and corderoite significantly decreases. Looking at these data, it is interesting to note that moving from the fraction <2 mm down to smaller particle sizes the amount of more crystalline Hg phases (especially corderoite and cinnabar) decreases, whereas higher quantities of Hg amorphous phase are found. It is known that amorphous phases are more soluble than crystalline ones, and that metacinnabar has a solubility which is higher than that of cinnabar (Mikac *et al.*, 2002). In addition, it is likely that sulfide solubility increases in the presence of Cl, as happens when cinnabar is converted to corderoite (Foord *et al.*, 1974; Paquette & Helz, 1995; McCormack, 2000; Spring & Grout, 2002; Cotte *et al.*, 2006; Terzano *et al.*, 2010). This speciation might also explain the high rate of Hg extracted in 6 *M* HCl where especially metacinnabar, corderoite and amorphous Hg forms can be solubilized. Highly insoluble cinnabar is usually found in the residual or can be partially extracted under oxidizing conditions (Sánchez *et al.*, 2005).

4. Conclusions

Even if Hg is speciated in quite insoluble forms, from the data presented it seems that the colloidal fraction, which is the most potentially mobile and thus the most dangerous, is enriched in relatively more soluble species, even if still quite resistant to extraction, as compared with cinnabar.

This aspect should be seriously taken into account when planning environmental risk assessment, since the small particle size in which Hg is concentrated and the changing speciation passing from millimetre to nanometre size could turn apparently safe conditions into more hazardous ones.

Soil analysis by synchrotron X-ray absorption spectroscopy allowed mercury speciation in the different soil fractions to be assessed and, in particular, the special features developed in this work for sample preparation and data collection for XANES analyses made it possible to speciate Hg in the submicrometre fractions even after the huge dilution to which the sample is subject during the SdFFF separation.

This research was partially financed by the MIUR (COFIN 2005) project 'Innovative chemical, physical and biological methods to characterize and remediate soils polluted by heavy metals (MICROS)'. The Institute of Synchrotron Radiation at FZK-Karlsruhe financially supported synchrotron experiments at ANKA. We thank Dr Melissa A. Denecke for her scientific support in data collection and elaboration at ANKA.

References

Bernaus, A., Gaona, X., Ivask, A., Karhu, A. & Valiente, M. (2005). *Anal. Bioanal. Chem.* **382**, 1541–1548.
Biester, H., Bindler, R., Martinez-Cortizas, A. & Engstrom, D. R. (2007). *Environ. Sci. Technol.* **41**, 4851–4860.
Biester, H., Gosar, M. & Covelli, S. (2000). *Environ. Sci. Technol.* **34**, 3330–3336.
Blo, G., Ceccarini, A., Conato, C., Contado, C., Fagioli, F., Roger, F., Pagnoni, A. & Dondi, F. (2006). *Anal. Bioanal. Chem.* **384**, 922–930.
Blo, G., Contado, C., Fagioli, F., Bollain Rodriguez, M. H. & Dondi, F. (1995). *Chromatographia*, **41**, 715–721.
Chittleborough, D. J., Hotchin, D. M. & Beckett, R. (1992). *Soil Sci.* **153**, 341–348.
Contado, C., Blo, G., Fagioli, F., Dondi, F. & Beckett, R. (1997). *Colloids Surf. A*, **120**, 47–49.
Cotte, M., Susini, J., Metrich, N., Moscato, A., Gratziu, C., Bertagnini, A. & Pagnao, M. (2006). *Anal. Chem.* **78**, 7484–7492.
Foord, E. E., Berendsen, P. & Storey, L. O. (1974). *Am. Mineral.* **59**, 652–655.
Giddings, J. C. (1993). *Science*, **260**, 1456–1465.
Gray, J. E. & Hines, M. E. (2006). *Appl. Geochem.* **21**, 1819–1820.
Hagemoen, S. W., Condemine, A. & Rockandel, M. A. (1994). *Chlorine Institute Annual Meeting*, Washington, DC, USA, 21–24 March 1994, P35-9403, pp. 1–5.
Hassellov, M., Lyvén, B., Bengtsson, H., Jansen, R., Turner, D. R. & Beckett, R. (2001). *Aquat. Geochem.* **7**, 155–171.
Lead, J. R. & Wilkinson, K. J. (2007). *Environmental Colloids and Particles: Behaviour, Separation and Characterization*, edited by K. J. Wilkinson and J. R. Lead, pp. 1–15. Hoboken: John Wiley and Sons.
McCormack, J. K. (2000). *Miner. Deposita*, **35**, 796–798.
Mikac, N., Foucher, D., Niessen, S. & Fischer, J.-C. (2002). *Anal. Bioanal. Chem.* **374**, 1028–1033.
Paquette, K. & Helz, G. (1995). *Water Air Soil Pollut.* **80**, 1053–1056.
Quejido, A. J., Cozar, J. S., Pérez del Villar, L., Galan, M. P., Crespo, M., Fernandez-Diaz, M. & Sanchez, M. (2002). *Trends Geochem.* **2**, 19–42.
Ranville, J. F., Chittleborough, D. J., Shanks, F., Morrison, R. J. S., Harris, T., Doss, F. & Beckett, R. (1999). *Anal. Chim. Acta*, **381**, 315–329.
Ravel, B. & Newville, M. (2005). *J. Synchrotron Rad.* **12**, 537–541.
Roberts, D., Nachtegaal, M. & Sparks, D. L. (2005). *Chemical Processes in Soils*, Vol. 8, *Soil Science Society of America Book Series*, edited by M. A. Tabatabai and D. L. Sparks, pp. 619–654. Madison: Soil Science Society of America.
Sánchez, D. M., Quejido, A. J., Fernández, M., Hernández, C., Schmid, T., Millán, R., González, M., Aldea, M., Martín, R. & Morante, R. (2005). *Anal. Bioanal. Chem.* **381**, 1507–1513.
Santoro, A., Terzano, R., Spagnuolo, M., Fiore, S., Morgana, M. & Ruggiero, P. (2010). *Int. J. Environ. Waste Manage.* **5**, 79–92.
Schuman, L. M. (2005). *Chemical Processes in Soils*, Vol. 8, *Soil Science Society of America Book Series*, edited by M. A. Tabatabai and D. L. Sparks, pp. 293–308. Madison: Soil Science Society of America.
Slowey, A. J., Johnson, S. B., Rhytuba, J. J. & Brown Jr, G. E. (2005). *Environ. Sci. Technol.* **39**, 7869–7874.
Spring, M. & Grout, R. (2002). *Natl. Gallery Tech. Bull.* **23**, 50–61.
Terzano, R., Santoro, A., Spagnuolo, M., Vekemans, B., Medici, L., Janssens, K., Göttlicher, J., Denecke, M. A., Mangold, S. & Ruggiero, P. (2010). *Environ. Pollut.* Submitted.
Webb, S. M. (2005). *Phys. Scr.* T**115**, 1011–1014.